PERGAMON

Electrochimica Acta 45 (2000) 1717–1725

ELECTROCHIMICA Acta

www.elsevier.nl/locate/electacta

In-situ spectroelectrochemistry (UV–visible and infrared) of anodic films on iron in neutral phosphate solutions

C. A. Borrás [a], R. Romagnoli [b], R.O. Lezna [c,*]

[a] *IMRE, Instituto de Materiales y Reactivos para la Electrónica, La Habana, Cuba*
[b] *CIDEPINT, Centro de Investigación y Desarrollo en Tecnología de Pinturas, Calle 52 entre 121 y 122, La Plata 1900, Argentina*
[c] *INIFTA, Facultad de Ciencias Exactas, Universidad Nacional de La Plata, Casilla de Correo 16, Sucursal 4, La Plata 1900, Argentina*

Received 30 March 1999; received in revised form 9 September 1999

Abstract

The composition of anodic films on iron formed at different potentials in neutral solutions has been investigated by in-situ UV–vis and IR spectroscopies in the presence of PO_4^{3-}, a non-contaminant inhibitor used in anticorrosive paints. Optical and electrochemical determinations were used to detect and characterize two well-defined current waves in the active region of Fe and a following passive zone at more positive potentials. The response has been associated with the presence on the surface, in the dissolution zone, of $Fe_3^{II}[PO_4]_2$ as the main species and probably some $[Fe^{III}PO_4]$. $[Fe^{III}PO_4]$ has been detected in the passive region by in-situ IR spectroscopy. Only minor amounts of Fe^{2+} and Fe^{3+} species in solution have been detected optically. These phosphated overlayers are believed to provide extra protective properties to the passivating film.

Keywords: Iron corrosion; Passivation; Coatings; Phosphate inhibitors; In-situ spectroscopy

1. Introduction

Inorganic phosphates have been used extensively as environmentally friendly corrosion inhibitors for iron and carbon steel surfaces in aqueous, nearly neutral solutions. Orthophosphates, in particular, are regarded as effective corrosion inhibitors and are classified as nonoxidizing anodic inhibitors in which the presence of oxygen is required for corrosion protection. During recent years, due to legal restrictions imposed upon chromate and lead pigments, zinc phosphate was incorporated to anticorrosive paints to attenuate base metal corrosion [1,2]. The role played by phosphates in this kind of paint is not yet fully understood [3,4]. A correct understanding of the mechanism through which passivity is achieved with phosphate could certainly help improve the performance of these pigments.

Kolotyrkyn et al. [5] assumed that in deaerated neutral phosphate solutions, a passivating monolayer of $Fe^{II}HPO4$ and a porous film of $Fe_3^{II}(PO_4)_2$ are formed. The protective film formed on iron in aerated phosphate solution was studied also by other authors [6,7] who found that this film is composed of a cubic oxide having the structure of Fe_3O_4, γ-Fe_2O_3 or an intermediate compound. Particles of ferric phosphate were also found embedded in the matrix of the cubic oxide.

Sato et al. [8,9] postulated that the anodic passivation film in acid solutions containing phosphates was an anhydrous oxide whereas in neutral and alkaline media there was an outer hydrated oxide layer influenced by pH and the anions present in solution. The oxide was assumed to be ferric.

* Corresponding author. Fax: +54-221-4530189.
E-mail address: rolezna@inifta.unlp.edu.ar (R.O. Lezna)

0013-4686/00/$ - see front matter
PII: S0013-4686(99)00393-X

Szklarska-Smialowska and Staehle [10] investigated protective films formed on iron in phosphate solutions as a function of pH. According to their view, films grown in deaerated Na_2HPO_4 solutions, probably $FeHPO_4$, are protective. They shift the potential to more positive values. Iron oxides are reported to form at high anodic potential together with iron phosphates leading to an enhanced protective capacity.

Corrosion of iron in somewhat similar systems has also been looked into by other authors who reported germane information to this study [11–16].

In-situ optical methods of high sensitivity (UV–vis and IR) allow detection of species on the electrode and generated at the iron electrode interface in aqueous solutions containing phosphate anions. The information is of importance to understand the protection mechanism afforded by phosphates. The aim of this preliminary research is to try to elucidate the nature of the protective films formed on iron in deaerated neutral phosphate solutions as a function of the applied potential. Measurements in the base electrolyte (i.e. without phosphates) were only taken for the sake of comparison.

2. Experimental

The working electrode for electrochemical experiments was a polycrystalline iron disc purchased from Johnson and Matthey (puratronic 99.9985%). The electrode diameter was 6 mm for polarization curves and UV–vis measurements and 11 mm for recording in-situ IR spectra. A platinum mesh, separated from the main compartment by a porous disc, was used as a counterelectrode. Prior to each experiment and just before getting the electrode into the solution a fresh surface was generated by polishing it to a mirror finish with alumina of particle size down to 0.05 mm followed by rinsing with Milipore Milli-Q water and sonication. Solutions were prepared with p.a. grade reagents sodium perchlorate and sodium dihydrogen phosphate adjusting the pH to 7.00 by means of sodium hydroxide solution. Potentials were measured and are quoted against a saturated calomel electrode (SCE) placed in a separate chamber and connected to the cell via a Luggin capillary. Oxygen was removed by bubbling purified nitrogen during for at least 30 min and, prior to each experience, the electrode was conditioned by holding it at -1.5 V during ca. 30 min to reduce fresh oxides.

Polarization curves were done at a positive scan rate of 1 mV s^{-1} or slower from -1.5 to $+1.5$ V employing two different electrolytes: 0.3 M sodium perchlorate (blank runs) and 0.3 M sodium perchlorate solution plus 0.1 M sodium dihydrogen phosphate, both of pH 7. Alternating current voltammograms were taken in the ± 1.5 V potential range with an exciting amplitude of 1.6 mV_{rms}/11 Hz, the sweep rate being 1 mV s^{-1} (single forward scan starting at -1.5 V).

2.1. UV–vis measurements

UV–vis spectra were obtained at an angle of incidence, ϕ, of 45°, using a computerized optical multichannel analyzer (EG&G PAR OMAIII) fitted with a cooled Si diode array [17]. The detector is unintensified and made up of 1024 channels. This rapid scan spectrometer, with a 14-bit resolution, was employed to obtain integral spectra resulting from the coaddition in computer memory of a variable number of exposures (depending on signal/noise), each averaged 0.03 s on the diode array chip. Diffraction orders higher than unity were sorted out by appropriate filters.

Spectra were collected during the progress of polarization curves. Iron species in solution formed at current maxima of the polarization curve were determined by means of suitable colorants such as dimethylglyoxime (DMG) for ferrous compounds and salicylic acid (SAL) for ferric species.

Spectra were taken by employing the set up described by using in this case a platinum electrode, at open circuit (OC), instead of iron. Unpolarized Pt worked merely as a radiation reflector. In all cases spectra were calculated as $(R-R_{ref})/R_{ref}$ with the reference spectra, R_{ref}, taken at appropriate potentials.

2.2. IR measurements

Infrared spectra were obtained in the range 1200 cm^{-1}/950 cm^{-1}. The electrochemical cell (for IR measurements) was designed with the aim of minimizing radiation losses by solvent (water) absorption. Therefore the iron electrode, flat, was tightly placed against an optical window (CaF_2 or ZnSe) so as to create a thin solution layer of a few microns. The technique consisted in the use of a high throughput dispersive spectrometer whose optics leads the radiation to the electrode at an angle of 60° for the CaF_2 window. The IR light is chopper modulated at 80 Hz while the potential is set to a fixed value or left at open circuit. The changes in the reflected intensity, ac signal R, are p-polarized and sensed by a narrow band, high sensitivity mercury–cadmium–telluride (MCT) detector. The output is rectified by a lock in amplifier, the final spectrum being, unless stated otherwise, the normalized difference between the optical response at a given potential against that at a potential taken as reference, R_{ref}, that is, $\Delta R/R_{ref}=(R-R_{ref})/R_{ref}$. The technique has been described in detail elsewhere [18–20]. A relatively high concentration of supporting electrolyte was used, 0.3 M $NaClO_4$, to eliminate phosphate bands that might appear as a result of potential dependent pH changes in the thin layer, which, in turn, may give rise to displacements of phosphate species equilibria [21].

3. Results and discussion

Neutral solutions, pH 7, were selected because it is the pH at which most phosphate-pigmented extracts and phosphate-based corrosion inhibitors operate, as stated previously.

Polarization curves in the base electrolyte show two main current maxima located at ≈ -0.3 and at ≈ -0.1 V with a shoulder at $+0.15$ V, Fig. 1B. In the case of phosphates + perchlorates the current maxima appeared at approximately the same potentials as the corresponding maxima of the blank solution although curve shapes and peak intensities are different in the presence of phosphates, Fig. 1A.

Ac voltammetry was carried out only to complement the information provided by polarization curves particularly to improve upon poorly resolved peaks (no impedance approach was intended). The main processes/peaks observed on polarization curves were found to respond to the modulation frequency employed, 11 Hz. The ac response is limited at the potential ends by the HER (hydrogen evolution reaction) at negative potentials, from -1.5 up to ≈ -0.8 V, and the oxygen evolution reaction (OER) at the positive extreme, beyond $+1.2$ V. Runs in the base electrolyte (Fig. 2a, 0.3 M $NaClO_4$), show in both the real and imaginary components a broad wave at -0.74 V probably arising from the adsorption of [OH^-] followed by another process starting at -0.6 V that gives rise to a couple of maxima at -0.3 and at -0.1 V. The ac current then falls off as the potential is made more positive showing a clear inflection at the beginning of passivation. A detail worth noticing on the cuadrature component of the blank run is the presence of a clear discontinuity at ≈ -0.39 V. The shape is characteristic of those arising from phase formation [22] signalling the appearing of an hydroxide or oxide on the surface. The first wave should correspond, in the base electrolyte, to the oxidation of Fe to give [$Fe(OH)_2$] on the surface and small amounts of Fe^{2+} in solution as detected by chemical analysis. [$Fe(OH)_2$] was then confirmed spectroscopically. The second wave may arise from the transformation of [$Fe(OH)_2$] into magnetite [F_3O_4] or [Fe_2O_3] [23–25].

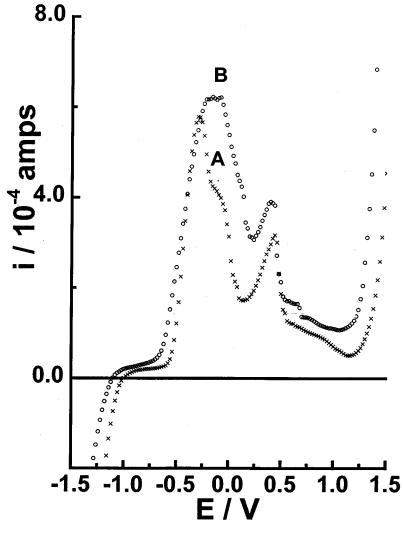

Fig. 1. Polarization curve of Fe at 1 mV s^{-1}, pH 7, initial potential = -1.5 V, deaerated solution. (A) 0.3 M $NaClO_4$ + 0.1 M $NaPO_4H_2$. (B) 0.3 M $NaClO_4$. Unless stated otherwise the electrode area was 0.28 cm^2.

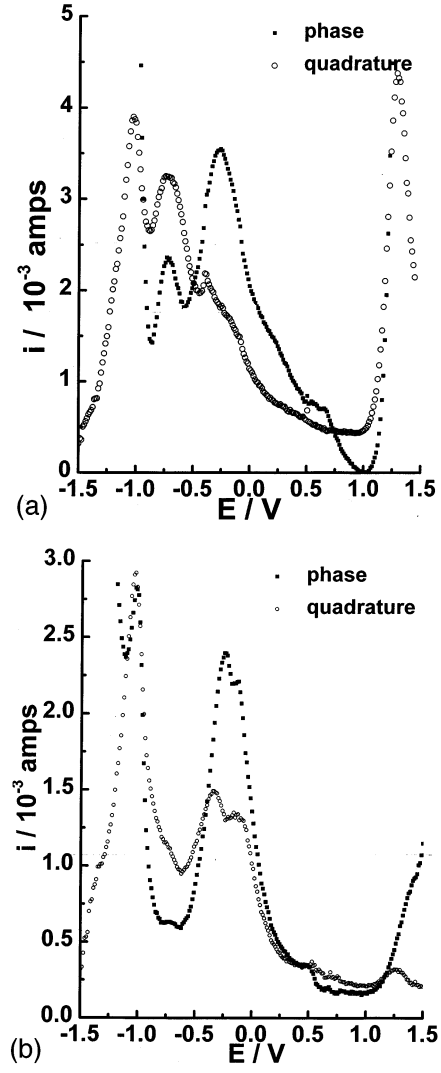

Fig. 2. (a) Alternating current voltammogram between -1.5 and $+1.5$ V of the Fe/0.3 M $NaClO_4$ interface, frequency 11 Hz, amplitude 1.6 mV_{rms}, $v = 1.00$ mV s^{-1} (single, forward scan). (b) Interface Fe/0.3 M $NaClO_4$ + 0.1 M $NaPO_4H_2$. Other conditions as in (a).

The response in 0.3 M $NaClO_4 + 0.1$ M $NaPO_4H_2$ (Fig. 2b), exhibits the influence of PO_4^{3-} at potentials as negative as -0.8 V where the sample curve starts diverging from that of the blank. Thus, the peak observed in the blank run at -0.74 V is barely visible with PO_4^{3-} in solution and no sign of phase transition can be detected. Two processes are detected at -0.3 and at -0.15 V, the one at -0.3 V being well-defined also on the imaginary component (capacitive). These two waves appear at roughly the same potentials as in the base electrolyte although with different intensities and shapes. In the presence of phosphates in solution the Fe species become phosphated giving rise mainly to $[Fe_3(PO_4)_2]$ on the surface as discussed in the next section. The current then gradually decreases to the potential where passivation sets in without any other feature on the trace. However, spectra and polarization curves indicate the presence of other important reactions between 0.0 and 0.6 V, attended by the formation of ferric species, such as $[Fe^{III}PO_4]$. These are probably slow processes that cannot follow the imposed ac perturbation.

The CV (dc) of a 0.3 M $NaClO_4 + 0.1$ M $NaPO_4H_2 + 5 \times 10^{-4}$ M Fe^{2+} suspension is presented in Fig. 3. The Fe^{2+}/Fe^{3+} couple can be observed at -0.37 V/$+0.17$ V, i.e. on the leading and trailing edges of the main two current peaks measured by ac/dc voltammetries.

The analysis of ac voltametry and steady-state measurements lead to an electrochemical response made up of three stages with, on the whole, a similar pattern to that obtained by other researchers at similar [26] or higher pHs [23].

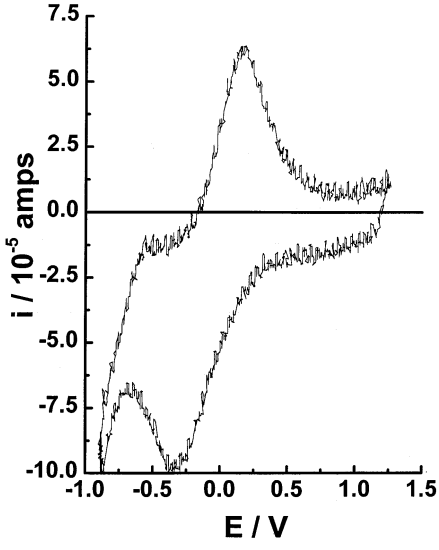

Fig. 3. Voltammogram of the Pt/0.3 M $NaClO_4 + 0.1$ M $NaPO_4H_2/5 \times 10^{-4}$ M Fe^{2+} suspension, $v = 50$ mV s^{-1}.

3.1. UV–vis spectra

The oxidation state of compounds in solution formed at the maxima of the dc/ac voltammetries was determined by complexing corrosion products with dimethylglioxime (DMG/Fe^{2+}) and salicylic acid (SAL/Fe^{3+}). DMG and SAL on their own present absorption bands at 362 and 327 nm, respectively.

The complex between DMG and ferrous ion absorbs at 530 nm. On the other hand the complex between SAL and ferrous ions is colorless. Ferric cation forms an amethyst color complex with SAL (534 nm) whereas the ferrous cation complex is colorless.

After the iron electrode had been polarized at -0.3 V during 4 min in the presence of DMG in solution (0.3 M $NaClO_4 + 0.1$ M $NaPO_4H_2$), an absorption band corresponding to the ferrous ion complex with DMG was detected while no coloration was observed with SAL. Therefore, it was concluded that only ferrous compounds in solution were formed at this potential.

On the other hand at $+0.42$ V, a weak and broad absorption band corresponding to the Fe(III)–SAL complex was observed.

Spectra, $\Delta R/R_{ref}$ versus λ, collected each at 100 mV during the progress of polarization curves, from -1.5 to $+1.5$ V at 1 mV s^{-1}, by employing 0.3 M $NaClO_4 + 0.1$ M $NaPO_4H_2$ as electrolyte, show featureless profiles for potentials negative to -0.5 V (-1.5 V reference, R_{ref}). Fig. 4 presents the spectra as from -0.3 V (top) to $+1.5$ V (bottom), plotted out each at 200 mV for the sake of clarity. A band peaked at 398 nm starts developing at -0.3 V whose intensity falls gradually into the red. The band shape remains mostly unchanged up to 0.0 V although it becomes more intense as the potential is made more positive. Between 0.0 V and $+0.7$ V the maxima are seen to shift to the red, up to ca. 570 nm, broadening the absorption shape. From $+0.3$ V onwards band intensities were observed to show a more sluggish growth. As from $+0.7$ V absorption intensities were observed to go over a maximun and then decrease rapidly. In order to determine the source of this change the signal, R, at $+0.3$ V was subtracted from the reflectance taken from $+0.5$ V onwards, that is $R_{ref} = R_{+0.3\,V}$. The resulting spectra, Fig. 5, plotted each at 200 mV as from $+0.5$ V (top), are positive in sign with a maximum at ca. 420 nm and tailing into the red, point to either the disappearance of absorbing species on the surface or their substitution by less-absorbing products. This interesting behaviour was noticed to continue up to $+1.3$ V, where the absorbance returned to negative values with respect to preceding spectra chosen as reference. We postulate $Fe_3^{II}[PO_4]_2$ as the species being replaced as from $+0.7$ V. The mineral Vivianit $Fe_3^{II}[PO_4]_2 \cdot 8H_2O$ is coloured strongly, generally green or yellowish green. On the other hand, samples prepared in our laboratory

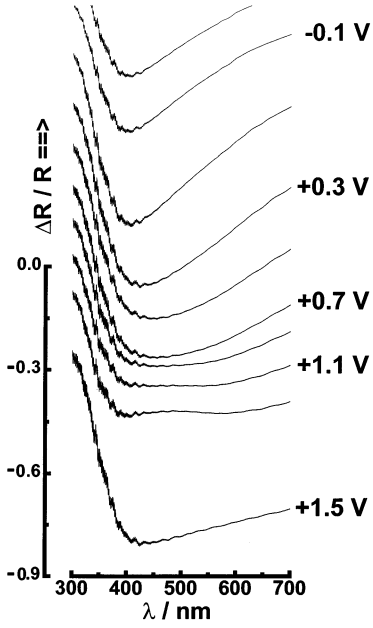

Fig. 4. $[(R - R_{-1.5\ V})/R_{-1.5\ V}]$ spectra plotted each at 200 mV between -0.3 and 1.5 V. R stands for reflectance. Electrolyte as in Fig. 1A. Spectra were averaged $10\times$ in memory, exposure time, 0.03 s, i.e. 300 ms per spectrum, angle of incidence $\phi = 45°$. Spectra were collected by a rapid scan spectrometer each at 100 mV during a positive-going linear potential sweep at 1 mV s^{-1} in the $-1.5 \rightarrow +1.5$ V potential range. Signal at -1.5 V, $R_{-1.5\ V}$, used as reference. For clarity only a spectra subset is shown.

of $[Fe^{III}PO_4]$, the likely substitute, were found to absorb radiation at shorter wavelengths than those of prepared $Fe_3^{II}[PO_4]_2$.

In the passive zone, between $+0.6$ and $+1.2$ V, a thick white–bluish layer was seen to develop on the surface. The ensuing augment in absorbance at potentials more positive than $+1.4$ V probably signals the onset of oxygen evolution.

The corresponding blank spectra (0.3 M $NaClO_4$), Fig. 6, exhibits a structure rather different to that of the sample in that only the intensity increases as the potential is made more positive whereas the shape does not change significantly. Between -0.4 and -0.2 V the spectra indicate maxima at ~ 380 and at 655 nm, Fig. 6 inset, values that coincide, in shape and energy, with those of the spectra for $Fe(OH)_2$ indicating the presence of this species on the surface. This signal was not detected in the presence of phosphates. $Fe(OH)_2$ is therefore observed on the spectra in the potential region where a current peak develops in the ac voltammetry (base electrolyte). No evidence of species disappearing or transforming was found in the blank run. The peak wavelengths for the rest of the curve, up to $+1.5$ V, stay close to 388 nm, with a long tail into the red region.

When the spectra for 0.3 M $NaClO_4 + 0.1$ M $NaPO_4H_2$ solutions are analized through peak intensity ($\Delta R/R < 0$) against potential diagrams at the set wavelengths of 388, 560, 660 nm, Fig. 7A and B, five potential regions with distinctive absorption properties can be observed. The wavelengths were selected to explore spectral regions instead of specific energies considering the 'bands' broad profiles in this system. Thus, 388 nm falls in the zone where the main absorption signals are detected for films developed with and without PO_4^{3-} in the electrolyte. The spectral region characterized by the formation and subsequently the disappearance of species with potential is sampled by radiation of 560 nm. The red corner, 660 nm, is explored mainly as a reference, as it presents no main bands except for the weak absorption arising from $Fe(OH)_2$ at negative electrode potentials. The spectrum at -1.5 V was taken as reference, $R_{ref} = R_{-1.5\ V}$. Thus, from -1.5 to -0.5 V the optical response is mainly flat with a small peak at -1.2 V. A sudden, broad increase in absorbance is observed between -0.4 and -0.1 V followed by a short plateau coinciding with the first peak in the ac voltammogram.

At -0.1 V, another less steep rise develops which levels off at $+0.2$ V paralleling the second maximun in the ac response. The two waves appear better defined in the blue than in the red region of the spectra. The curve at 560 nm is interesting in that it confirms there is a

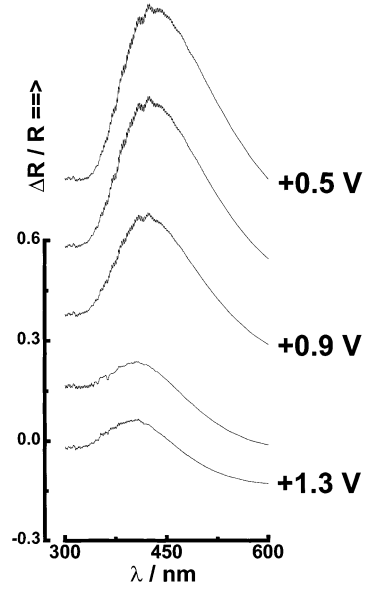

Fig. 5. $[(R - R_{+0.3\ V})/R_{+0.3\ V}]$ spectra shown each at 200 mV between 0.5 and 1.3 V. The reference spectrum at $+0.3$ V was chosen to emphasize the disappearance of species absorbing at ca. 420 nm. Notice + sign on Y axis. Potentials labeled each at 400 mV. Electrolyte as in Fig. 1A. Experimental condition as in Fig. 4.

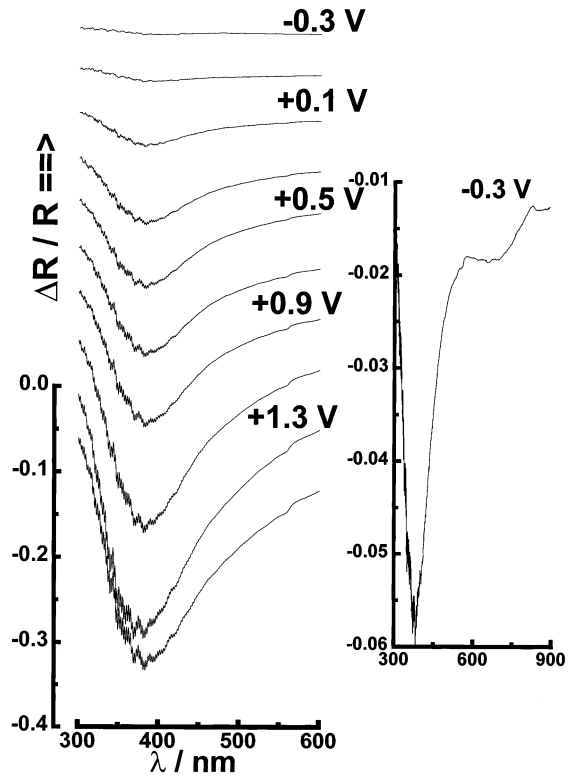

Fig. 6. Set of blank spectra plotted each at 200 mV. Measuring potentials indicated each at 400 mV above the corresponding curves. Electrolyte as in Fig. 1B. Other conditions as in Fig. 4. Inset: spectrum taken at -0.3 V, assigned to $[Fe(HO)_2]$. Inset axes labels as in main graph.

species whose absorbance starts decaying at intermediate potentials, between ca. $+0.2$ and $+0.7$ V. From $+0.7$ up to $+1.2$ V there is rapid decrease in peak intensity at all wavelengths, i.e. the film becomes less absorbing. On the other hand, the corresponding plots, e.g. at 388 nm, for the base electrolyte, Fig. 7B, 0.3 M $NaClO_4$, present two poorly-defined waves on top of an increasing absorbing curve up to $+1.3$ V. Similar shapes have been reported by Kruger et al. [26], at the same pH, for diagrams of thickness versus charge during the growth of iron oxides. The main difference with respect to solutions containing phosphates, appart from that of intensity, lies with the passive region, $+0.7$ V/1.3 V, where there is a strong decrease in absorbance in the presence of phosphates whereas a continuos increase is detected in the base electrolyte.

3.2. IR spectra

In-situ IR spectra were taken of passivated samples at open circuit, normalized to a reference obtained at -1.5 V of an oxide-free electrode in the same solution. Passivation was achieved by holding the potential at $+1.0$ V (electrode away from optical window) after a potential step from -1.5 V, the potentiostat being switched out after ca. 20 min at which time the current had gone down to a minimum, steady-state value. The collection of spectra was started immediately afterwards with the electrode at the window.

The IR spectrum of a 1 M $NaPO_4H_2$ solution was measured in the electrochemical cell by using a gold electrode (unpolarized) as a reflector and a ZnSe optical window. The objective was to identify species in solution. Two bands were observed at 988 and 1077 cm^{-1} as reported in the literature for the species $[HPO_4^{2-}]$ in solution, Fig. 8 inset E. At concentrations lower than 1

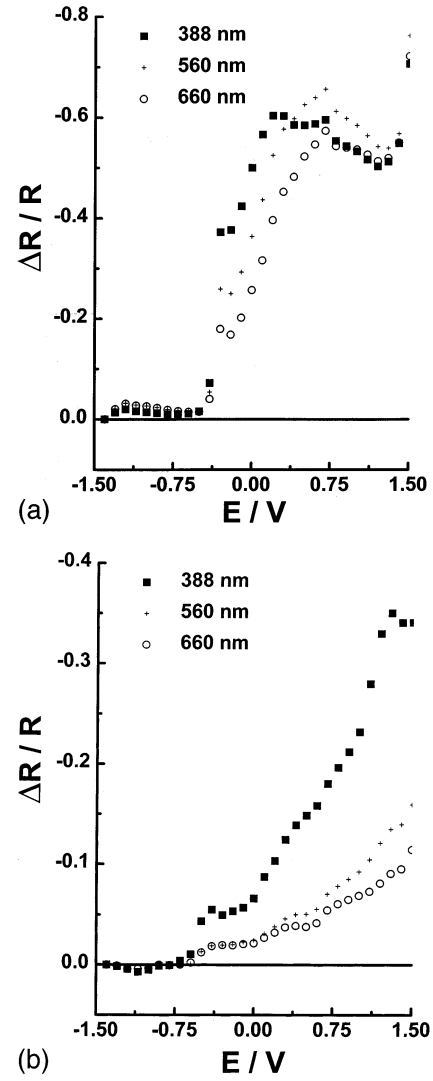

Fig. 7. Band (peak) intensity at set wavelengths against potential. Reference spectrum taken at -1.5 V. (A) 0.3 M $NaClO_4 + 0.1$ M $NaPO_4H_2$. (B) 0.3 M $NaClO_4$. Wavelengths selected to match regions of main features in blank/sample spectra.

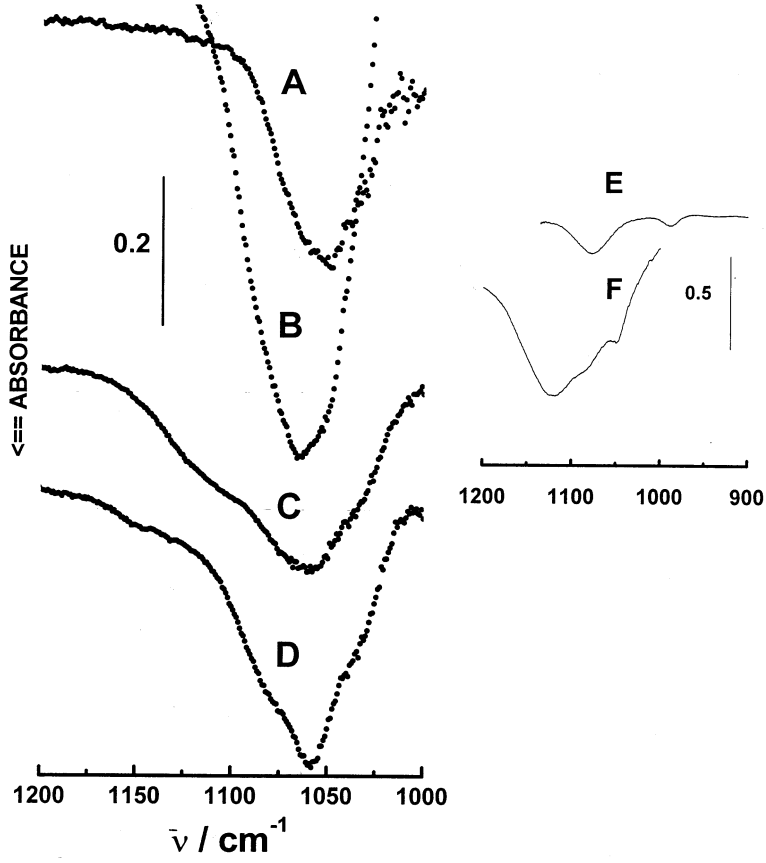

Fig. 8. In-situ IR spectra of passive films on Fe taken at open circuit. Signals shifted vertically for a better view. Curves (A, C and D) correspond, in the three cases, separate experiments, to layers formed at +1.0 V in 0.3 M $NaClO_4$ + 0.1 M $NaPO_4H_2$ following a potential step from −1.5 V. Spectra of films measured in oxygen-free water. Reference was the oxide-free Fe electrode in oxygen-free water. Trace (B) was taken, at open circuit, after a polarization curve at 1 mV s^{-1} spanning the same potential range, −1.5→+1.5 V, spectrum of film in 0.3 M $NaClO_4$ + 0.1 M $NaPO_4H_2$. Reference measured at −1.5 V. Electrode area: 0.95 cm^2. Inset: (E) solution spectrum (1 M $NaPO_4H_2$), radiation reflected off an unpolarized gold electrode (ZnSe window). (F) In-situ IR of the system Fe/0.3 M $NaClO_4$ taken at open circuit after a polarization curve at 1 mV s^{-1} between −1.2 and +1.5 V. Reference measured at −1.2 V (CaF_2 window). Inset axes labels as in main graph.

M, the signals from phosphate species in solution came out rather weakly, therefore indicating their contribution at 0.1 M would be almost negligible. However, to further eliminate possible contributions from species/products in solution or trapped in the thin layer between electrode and optical window, some experiments were carried out as follows, after forming the passivating film in 0.3 M $NaClO_4$ + 0.1 M $NaPO_4H_2$, the solution was exchanged with deoxygenated distilled water before scanning the film spectrum. The corresponding reference was obtained also in oxygen-free distilled water by using a fresh polished electrode. The optical cell was not moved during the manipulation. The data taken of films in water were found in good agreement with those gathered in the supporting electrolyte. Spectra are plotted as $\Delta A = -\ln[1 + \Delta R/R_{ref}]$ versus $\bar{\nu}$ (wavenumbers). Fig. 8A, C and D show the most reproducible shapes for the spectrum, in water, of a film grown in separate experiments at +1.0 V in 0.3 M $NaClO_4$ + 0.1 M $NaPO_4H_2$ after a potential step from −1.5 V. The trace in Fig. 8B, on the other hand, corresponds to the spectrum in the supporting electrolyte (ClO_4^- + PO_4^{3-}), of the anodic film grown on Fe at the positive end of a polarization curve between the same potential limits, −1.5 V/+1.0 V. Passivated layers obtained after potential steps are made up of products formed at a single potential, whereas passivated films found at the end of polarization curves are supposed to contain species formed/transformed all along the curve. Band positions are, however, not much different for the two cases, although band shapes may be distinct.

The frequencies, average over several spectra, not only those in the diagram, lead to 1050, 1062, 1080,

1092, 1110 cm^{-1} plus a shoulder at 1025–1030 cm^{-1} as the most reproducible values. Although frequencies were reproducible, intensities were found to vary from one experiment to the next. No iron oxides/hydroxides IR bands are expected in this region. The spectrum of the base electrolyte, 0.3 M $NaClO_4$, is included as an inset (F) to Fig. 8. The response in this case is dominated by the ClO_4^- signature which accumulates on the solution side of the interface because of the electrode positive charge.

The fact that the IR spectra of $Fe_3^{II}[PO_4]_2$ and $[Fe^{III}PO_4]$ are rather similar makes their differentiation somewhat difficult. Vibrations, on average at 1096 and 1044 cm^{-1}, ν(P–O), have been reported for surface phosphate complexes such as $\equiv Fe^{III}PO_4$ on α-$Fe^{III}OOH$ [27] in the same pH range. However, we are mainly dealing with thick deposits. Therefore, their properties should be better compared with those of bulk $[FePO_4]$. Ferric phosphates have got IR bands at 1050 and 1100 cm^{-1} that, although broad signals, are in good agreement with our findings[28]. The possibility that some of the frequencies detected might arise from $[Fe_3^{II}(PO_4)_2]$ seems unlikely as we did not find any absorption at ca. 990 cm^{-1} (ZnSe optical window), as should be expected if ferrous phosphate were in the layer [29]. Moreover, the disappearance of this species, $[Fe_3^{II}(PO_4)_2]$, was observed through the UV–vis spectra at the start of passivation, vide supra. Therefore we propose $[Fe^{III}PO_4]$ as the most likely species giving rise to the IR spectra observed in the passive zone.

4. Conclusions

The analysis of the whole set of data, optical and electrochemical in the base electrolyte, point to the formation of $[Fe(HO)_2]$ on the surface at negative potentials, ~ -0.3 V, probably preceded by the adsorption of OH^- that takes place once the Fe surface becomes free of hydrogen. The onset of the new phase gives rise to a maximun on absorption/current curves as a function of potential. A second arrest at -0.15 V can be assigned to the formation of magnetite, $[Fe_3O_4]$, as has been reported in Raman studies [23]. $[Fe_2O_3]$, with a broad absorption band at ca. 500 nm, could also be a likely assumption for the species formed.

As has been consistently reported in the literature [5–7,15,16], the passivation of iron is believed to be attended by the formation of Fe^{3+} species, such as FeOOH or γ-Fe_2O_3 , on top of magnetite through the oxidation of $[Fe(HO)_2]$ or $[Fe_3O_4]$ itself.

The presence of phosphates in the system alters the system drastically as the Fe surface species become phosphated even at negative potentials (-0.8 V), that is, in the zone where $[Fe(HO)_2]$ has been detected in the base electrolyte. The main species in the potential region prior to passivation should then be $[Fe_3^{II}(PO_4)_2]$, which has got a colour in the green/yellow region. $[Fe_3^{II}(PO_4)_2]$ with a broad band at ca. 420 nm, tailing into the red, was observed to start disappearing at ca. $+0.4$ V to be replaced by a thick white deposit of $[Fe^{III}(PO_4)]$. The presence of $[Fe^{III}(PO_4)]$ in the passive film has been further suggested by its absorption in the 1000–1200 cm^{-1} region of mid-infrared.

Acknowledgements

This work was supported by grants by CONICET (RA) and CIC (Province of Buenos Aires, RA). The authors wish to thank The Third World Academy of Sciences (TWAS) for a travel grant given to C.A.B. Technical assistance by E. Fernández is gratefully acknowledged.

References

[1] A. Gerhard, A. Bittner, J. Coat. Technol. 58 (1986) 59.
[2] A. Bittner, J. Coat. Technol. 61 (1989) 111.
[3] G. Meyer, Farbe + Lack 71 (1965) 113.
[4] R. Romagnoli, V.F. Vetere, Corrosion (NACE) 51 (1995) 116.
[5] Ja.M. Kolotyrkin, Ju.A. Popov, A.A. Vasilev, Elektrokhimia 9 (1855) 1973.
[6] J.E.O. Mayne, J.W. Menter, J. Chem. Soc. (1954) 103.
[7] M.J. Pryor, M. Cohen, J. Electrochem. Soc. 100 (1953) 203.
[8] N. Sato, T. Noda, K. Kudo, Electrochim. Acta 19 (1974) 471.
[9] N. Sato, K. Kudo, T. Noda, Corr. Sci. 10 (1970) 785.
[10] Z. Szklarska-Smialowska, R.W. Staehle, J. Electrochem. Soc. 121 (11) (1974) 1393.
[11] R.D. Armstrong, I. Baurhoo, J. Electroanal. Chem. 34 (1972) 41.
[12] R.D. Armstrong, I. Baurhoo, J. Electroanal. Chem. 40 (1972) 325.
[13] S. Juanto, R.S. Schrebler, J.O. Zerbino, J.R. Vilche, A.J. Arvia, Electrochim. Acta 36 (1991) 1143.
[14] H. Zhang, Su.M. Park, J. Electrochem. Soc. 141 (3) (1994) 718.
[15] T. Piao, Su.M. Park, J. Electrochem. Soc. 144 (10) (1997) 3371.
[16] P.A. Christensen, A. Hamnett, in: Techniques and Mechanisms in Electrochemistry, Chapman and Hall, London, 1994, p. 325 and references therein.
[17] R.O. Lezna, S. Juanto, J.H. Zagal, Electroanal. Chem. 389 (1–2) (1995) 197.
[18] B. Beden, C. Lamy, J.-M. Léger, in: J.M. Bockris, B.E. Conway, R. White (Eds.), Modern Aspects of Electrochemistry, vol. 22, Plenum Press, New York, 1992, p. 97.
[19] R.O. Lezna, K. Kunimatsu, T. Ohtsuka, N. Sato, J. Electrochem. Soc. 134 (12) (1987) 3090.
[20] R.O. Lezna, An. Asoc. Quím. Argent. 82 (4) (1994) 293.

[21] T. Iwasita, F.C. Nart, H. Polligkeit, Ber. Bunsenges. Phys. Chem. 95 (5) (1991) 638.
[22] F.G. Thomas, Cl. Buess-Herman, L. Gierst, J. Electroanal. Chem. 214 (1986) 597.
[23] A. Hugot-Le Goff, J. Flis, N. Boucherit, S. Joiret, J. Wilinski, J. Electrochem. Soc. 137 (9) (1990) 2684.
[24] C.T. Chen, B.D. Cahan, J. Electrochem. Soc. 129 (1) (1982) 17.
[25] R.G.J. Strens, B.J. Wood, Miner. Mag. 43 (1979) 347.
[26] J. Kruger, J.P. Calvert, J. Electrochem. Soc. 114 (1) (1967) 43.
[27] M.I. Tejedor-Tejedor, M.A. Anderson, Langmuir 6 (1990) 602.
[28] Sadtler Research Laboratories, Inc., Philadelphia, PA, USA, 1965.
[29] H. Moenke, Mineralspektren, Table 5.24, Akademie–Verlag, Berlin, 1962.